

Constrained Impulsive Trajectory Optimization for Orbit-to-Orbit Transfer

Richard G. Brusch*

General Dynamics Convair Division, San Diego, Calif.

A method for rapidly generating preliminary estimates of performance for orbit-to-orbit transfer vehicles subject to complex operational constraints is presented. Given the characteristics of a particular multistage design and the position and time of the thrusting arcs, the performance index and constraints are evaluated by solving Lambert's problem. An intrinsic equality constraint is imposed on each thrusting arc to insure that the velocity increment provided by each stage is equal to the impulsive velocity increment required by the solution to Lambert's problem. A problem solution is sought by solving a nonlinear programming problem where the independent variables may be chosen from a set of vehicle design parameters and the positions and times of the various thrusting arcs. A Lambert's problem formulation is shown to be preferable to a Kepler's problem formulation for complex missions. Pitfalls in the solution to Lambert's problem are highlighted. A variation of the Method of Multipliers is used for reliably solving the nonlinear programming problem generated by the problem formulation. Finally, several highly constrained orbit-to-orbit transfer problems are presented as examples.

Introduction

OPTIMIZATION of trajectories for orbit-to-orbit transfer has recently been complicated by the fixed impulses available from upper stages using solid rocket motors, such as the Interim Upper Stage (IUS) proposed for use with the space shuttle. Furthermore because of development costs, only a few solid-rocket-motor upper stages will be available, each with a discrete total impulse capability. It is clearly necessary then to perform many missions with stages that are poorly sized from an impulse available standpoint. The question then becomes one of optimizing trajectory design, given poorly sized stages. The trajectory shaping techniques that work well for liquid-propellant stages, such as Hohmann transfers, cannot be used because of the total impulse constraints imposed by the use of solid-rocket-motor stages. This problem was the major motivation for developing the technique described in this paper.

A second motivation was the need to solve orbit-to-orbit transfer problems requiring three or more impulses. Analytical solutions to these problems are unavailable even for multiburn liquid-fuel stages, such as the Agena, Centaur, and Transtage, where fixed impulse constraints are not a problem. For problems requiring a change of the size or shape of the orbit as well as the orbital plane, three impulse transfers are frequently optimal and, to the best of the author's knowledge, solutions may be obtained only through some numerical iteration procedure.

Preliminary performance estimation tools should have the attributes of rapid response, flexibility, and low cost. Trajectory optimization programs that integrate the equations of motion¹⁻⁴ usually fail to meet the last criterion due to the relatively high cost of trajectory integration multiplied by the number of trajectories that must be computed in the solution iteration process. In these programs, the solution iteration overhead is infinitesimal compared with trajectory integration

costs. Therefore, lowering the cost of trajectory propagation is an obvious approach to developing a viable preliminary performance estimation tool.

Impulsive approximation of finite-burn arcs and conic approximation of coast arcs offer the potential of reducing trajectory propagation costs by two to three orders of magnitude over that required by numerical integration. By choosing an adequate number of impulses to simulate a single finite burn, even trajectories with relatively low thrust-to-weight ratios (≈ 0.1) and long thrusting arcs may be simulated with sufficient accuracy for preliminary performance estimation work. The paper of Gobetz and Doll offers an excellent survey of impulsive trajectories.⁵

Impulsive thrust approximations and conic coast propagation are treated in the following sections. The next portion of the paper discusses a variation of the Method of Multipliers developed by the author for reliably solving the nonlinear programming problem generated by the problem statement. Finally, several example problems and solutions are presented to indicate the value of this approach.

Impulsive Burn Approximation

Consider a vehicle moving in a constant gravitational field and thrusting in a constant direction from time t_0 to time t_f . It can be shown from simple dynamics that the velocity change relative to a free-falling coordinate system due to the finite burn is equivalent to an impulse having the same characteristic velocity Δv and occurring at the time centroid t_c of the thrust acceleration $a(t)$ versus time profile

$$0 = \int_{t_0}^{t_f} (t - t_c) a(t) dt \quad (1)$$

$$\Delta v = \int_{t_0}^{t_f} a(t) dt \quad (2)$$

The maneuvers are equivalent in the sense that they both start on the same preburn coast trajectory and end on the same postburn coast trajectory. This equivalence is illustrated in Fig. 1 for a rocket with constant thrust F and constant weight flow rate \dot{w} . With these assumptions, Eq. (1) can be

Received Jan. 24, 1978; revision received July 28, 1978. Copyright © American Institute of Aeronautics and Astronautics, Inc., 1978. All rights reserved.

Index categories: Earth-Orbital Trajectories; Spacecraft Navigation, Guidance, and Flight-Path Control; LV/M Mission Studies and Economics.

*Senior Engineering Specialist, Systems Analysis. Member AIAA.

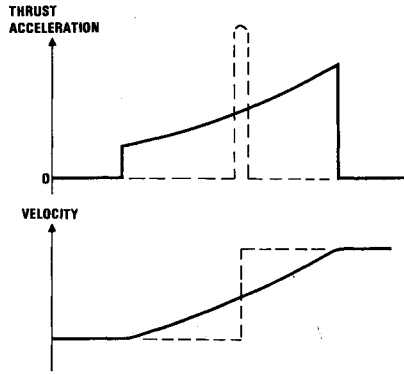


Fig. 1 Equivalent finite burn (solid line) and impulse maneuvers.

solved explicitly for the time of the thrust acceleration centroid, given the initial weight w_0

$$t_c = t_0 + w_0 / \dot{w} - (t_f - t_0) / \ln R \quad (3)$$

where

$$R = w_0 / w_f \quad (4)$$

$$w_f = w_0 - \dot{w}(t_f - t_0) \quad (5)$$

are the mass ratio and final weight, respectively.

The inexactness of this impulsive approximation is due to violation of two of the assumptions by actual trajectories: 1) a nonuniform gravity field due to changes in radius during the finite-burn maneuver, and 2) thrust vector turning during the burn. Reference 6 has investigated the performance errors induced by ignoring these factors; the results are summarized by the following bound on the difference between the impulse characteristic velocity Δv and the finite-burn characteristic velocity Δv_f :

$$\Delta v_f - \Delta v \leq k(1/24)(\mu/r^3)(t_f - t_0)^2 \Delta v \quad (6)$$

where

$$k = \frac{6}{q} \left(\coth \frac{q}{2} - \frac{2}{q} \right) = 1 - \frac{1}{60} q^2 + \frac{1}{2520} q^4 - \dots \quad (7)$$

and r is the radius to the center of mass, μ is the gravitation constant of the center of mass, and q equals Δv divided by the effective exhaust velocity.

For burns imparting a velocity change less than the effective exhaust velocity, setting k to unity will result in an error of less than 2% in the bound of Eq. (6). Equation (6) provides a straightforward means of determining the maximum burn duration that can be approximated by a single impulse given an upper bound on the tolerable error in characteristic velocity. For example, if an error of 0.1% in characteristic velocity is considered negligible, then solving Eq. (6) for the maximum allowable burn duration yields

$$t_f - t_0 = [0.001 \times 24(r^3/\mu)/k]^{1/2} \quad (8)$$

If the burn time of the finite burn exceeds this value, the error tolerance requirements can still be met by modeling the burn by two or more sequential impulses, each representing an equal portion of the total finite burn. This approach is followed in this paper. An alternative approach is to use a more sophisticated impulsive approximation, such as a position translation orthogonal to the impulse at the impulse point suggested by Robbins in Ref. 6.

Conic Coast Approximation

Consider now the problem of obtaining approximate solutions to the unpowered or coasting phases of flight, the

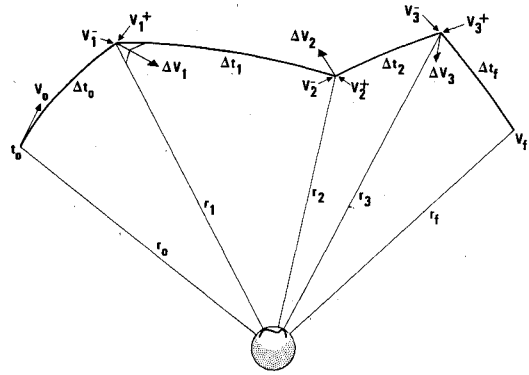


Fig. 2 A general three-impulse transfer in three-dimensional space.

so-called "two-body" problem. If all forces except a spherical inverse squared gravitational field are ignored, elegant analytic solutions are available. Note that the following forces are ignored in accepting the previous assumption: 1) higher-order gravitational harmonics, 2) atmospheric drag, 3) the solar wind, and 4) third-body gravitational perturbations. The first two of these can have a significant effect on low Earth orbits, especially when multiple revolutions are involved. Higher-order gravitational harmonics are briefly treated at the end of this section.

Although many "two-body" problems can be posed, the analytic solutions to the following two practical problems are of greatest interest: 1) the problem of Kepler is to determine the position and velocity vectors r_f and v_f at some future time t_f , given the position and velocity vectors r_0 and v_0 at the present time t_0 ; and 2) the problem of Lambert is to determine the initial and final velocity vectors v_0 and v_f , given the initial and final position vectors r_0 and r_f and a transit time, $t_f - t_0$.

Kepler's Problem

An excellent practical solution to Kepler's problem has been presented by Goodyear.^{7,8} The solution to Kepler's problem is straightforward and without ambiguities. A general multiple-burn trajectory in three-dimensional space is shown in Fig. 2. The natural control variables of this approach to trajectory propagation are the initial position and velocity vectors r_0 and v_0 and the coast times between impulses Δt_i and the impulse vectors Δv_i . For this particular example,

$$x = [r_{01}, r_{02}, r_{03}, v_{01}, v_{02}, v_{03}, \Delta t_0, \Delta v_{11}, \Delta v_{12}, \Delta v_{13}, \Delta t_1, \Delta v_{21}, \Delta v_{22}, \Delta v_{23}, \Delta t_2, \Delta v_{31}, \Delta v_{32}, \Delta v_{33}, \Delta t_3] \quad (9)$$

where x denotes the vector of all scalar control variables. A general trajectory then is completely determined by the vector of control parameters x . Notice that four additional control variables are added for each additional impulse incorporated. Equivalently, the three components of the Δv_i vectors may be replaced by the magnitude of the impulse $\|\Delta v_i\|$ and two coordinates that uniquely specify the orientation of the impulse vector; e.g., spherical coordinates.

Lambert's Problem

An alternative approach to trajectory propagation is to specify the position vectors of the impulses and the transfer times between impulses and solve for the initial and final velocity vectors. For additional flexibility, the formulation presented here will allow the possibility of an initial coast before the first impulse and a final coast after the last impulse. These initial and final coasts will be determined using a solution to Kepler's problem while all transfers between impulse will be determined from a solution to Lambert's problem. Numerical techniques for solving Lambert's

problem are discussed in Ref. 9-12. In this formulation, the natural control variables are the coast times Δt_i , the position vectors r_i , the initial velocity v_0 , and the velocity prior to the final coast v_3^+ .

$$x = [v_{01}, v_{02}, v_{03}, r_{01}, r_{02}, r_{03}, \Delta t_0, \Delta t_1, r_{21}, r_{22}, r_{23}, \Delta t_2, r_{31}, r_{32}, r_{33}, v_{31}, v_{32}, v_{33}, \Delta t_f]$$

Notice that r_f is not present in the control vector since it is determined by the initial coast. As in the case of the Kepler problem formulation, four additional control variables are added for each additional impulse. Notice that each impulse vector now can be computed from $\Delta v_i = v_i^+ - v_i^-$.

Comparison of Formulations

Notice that both the Kepler problem formulation and the Lambert problem formulation of this general three-impulse trajectory with initial and final coasts have the same number of control variables, 19; they both have the same number of degrees of freedom, which may be subject to optimization. From this standpoint, they are equivalent in complexity. Constraints on the magnitude of the impulses may be more easily enforced in the Kepler problem formulation since the impulses appear as control variables. However, for multiple-burn liquid-fuel rockets, the optimal impulse magnitudes are not known a priori and the advantage is lost.

Both approaches require initial estimates of the control variables to begin optimization iterations. For the Kepler problem formulation, the initial orbital elements, the coast times between impulses, and the magnitude and direction of each of the impulses must be guessed. For the Lambert problem formulation, the initial and final orbital elements, the coast times, and the positions of each impulse must be estimated. The initial and final orbits are frequently part of the problem statement. In our opinion, it is much easier to guess the position of impulses than to guess the magnitude and especially the direction of impulses. A trajectory analyst has a much better sense for where an impulse will occur than he does for the direction of the impulse in a three-dimensional inertial coordinate system. In the Lambert formulation, all iterations, including the initial estimate, achieve the desired terminal orbit; this is not the case for the Kepler problem formulation.

The most persuasive argument favoring the Lambert problem formulation is one based on error propagation and numerical stability. Changing a single control variable when using Kepler's formulation changes the entire trajectory following the impulse associated with that parameter. Consequently, the trajectory will be much more sensitive in general to variations in r_0 and v_0 than to variations in Δt_f . The longer and more complex the trajectory to be simulated, the more severe this sensitivity problem becomes. For missions such as rendezvous in geosynchronous orbit from a low Earth orbit, followed by a return to low Earth orbit, a variation in the elements of the initial parking orbit can cause variation four or five orders of magnitude larger in the final orbit. Such a problem is poorly conditioned for the generation of gradients by finite differences. Also function minimization algorithms require more computational effort due to the extreme cross-coupling among control variables.

A variation of a parameter in the Lambert problem formulation can only affect the two coast arcs adjacent to the impulse position or time being varied. Thus, a parameter variation affects only three contiguous Δv vectors. The sensitivities are therefore more uniform and local, improving finite-difference gradients; and the limited cross-coupling of control variables improves function minimization algorithm performance.

During development of the program described in this paper, the author attempted several problems using both formulations. The Lambert problem formulation was able to

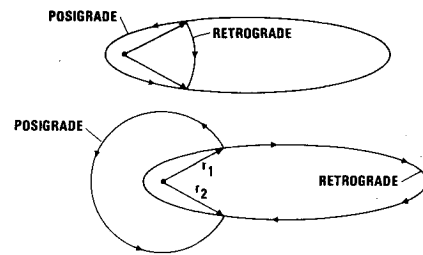


Fig. 3 A clockwise and counterclockwise solution to Lambert's problem always exists.

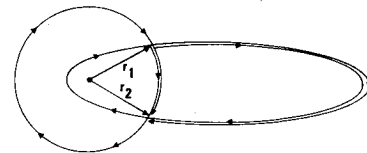


Fig. 4 Two possible solutions to Lambert's Problem with a central angle greater than 360 deg.

converge to significantly more accurate solutions than the Kepler problem formulation. The cause of the difference in performance was traced to a significant degradation of accuracy in the finite-difference gradients that could be obtained with the Kepler formulation. Although the gradient accuracy could be improved by going to double precision, the ill-conditioning due to cross-coupling of control variables and the wide range of magnitudes of components of the gradient vector are inherent in the problem formulation.

Similar problems occur in the solution of two-point boundary-value problems involving sensitive "divergent systems of differential equations." The Kepler formulation is analogous to the "shooting" technique used on the differential equation problem. The Lambert problem formulation is akin to the "multiple shooting" approach, which has been used successfully to solve sensitive differential equations.¹³

Ambiguities of Lambert's Problem

Unfortunately, the solution to Lambert's problem is not as straightforward as the solution to Kepler's problem. Lambert's problem suffers from a number of intrinsic ambiguities:

1) Given two position vectors and a transfer time, two solutions are always possible—a clockwise solution, and a counterclockwise solution (see Fig. 3).

2) For transfer times Δt greater than the period P_{\min} of the minimum-energy ellipse determined by the position vectors, solutions with total central angles greater than 360 deg are possible in addition to the solutions with central angle less than 360 deg (see Fig. 4). In fact, two posigrade and two retrograde solutions are possible with central angles between $2\pi n$ and $2\pi(n+1)$ when the transfer time is sufficiently large.

3) If vectors r_1 and r_2 are collinear (parallel, although possibly with opposite sense) the plane of the transfer is undefined. This includes the important practical cases when impulses are positioned 180 or 360 deg apart. These cases correspond to perigee-apogee impulse combinations known to be optimal for Hohmann transfers or to successive apogee or successive perigee burns, frequently optimal maneuver when finite thrust limits available impulse magnitudes.

The multiple solutions posed by ambiguities 1 and 2 can frequently be dispensed with on the grounds of common sense arguments or other mission considerations. For example, if the angle between the planes of the initial and final orbits is small and motion is intended to be posigrade in both orbits, a retrograde transfer orbit will be extremely uneconomical from

a Δv standpoint and would make sense only if stages performing the transfer were extremely oversized relative to stages designed to perform the minimum-energy transfer. Some candidate solutions may violate minimum perigee constraints (aerodynamic heating or impact), eliminating them from further consideration. Often, multiple-revolution trajectories are eliminated from consideration on the grounds of increased weight (larger batteries, more vehicle stabilization propellants) or the cost of ground support required by increased mission duration. In some cases, however, the only recourse is to optimize the transfer relative to each transfer mode and select the optimum mode based on the direct comparison of the optimum performance achieved by each mode. Note that only a finite number of cases need be tried; however, as the number of impulses increases, the number of possible combinations increases exponentially. Note that the problem of alternate mission modes is shared by all problem formulations.

The problem of collinear position vectors is a more serious one because it occurs more frequently in practice and because an infinite number of solutions exists, corresponding to the continuum of possible transfer plane orientations. It should be noted, however, that constraints, particularly stage impulse constraints associated with solid-fuel rocket motors, frequently force the solution away from the Hohmann transfer case. Still, provisions must be made to handle this case when it occurs. Rocklin¹¹ has investigated this problem for the two-impulse case when the performance index is defined as the sum of magnitudes of the velocity increments, and no constraints are imposed other than the given initial and final position and velocity vectors. He concludes that

$$\Delta v_0 \cdot h_i / (r_0 \|\Delta v_0\|) = -\Delta v_f \cdot h_i / (r_f \|\Delta v_f\|)$$

$$\theta = (2n+1)\pi \quad (10)$$

and

$$\Delta v_0 \cdot h_i / \|\Delta v_0\| = \Delta v_f \cdot h_i / \|\Delta v_f\|$$

$$\theta = 2n\pi \quad (11)$$

$$(v_2 \Delta v_{f1} - v_1 \Delta v_{f2}) / \|\Delta v_f\| = (v_2 \Delta v_{01} - v_1 \Delta v_{02}) / \|\Delta v_0\|$$

$$(n=0,1,2,\dots) \quad (12)$$

where h_i is the unit angular momentum vector of the transfer orbit; subscripts 1,2,3 refer to components in an orthogonal coordinate system with x_1 and x_2 in the plane of the transfer orbit; the x_1 axis in the direction of periapsis, and the x_3 axis in the direction of the angular momentum vector. Subscripts 0 and f refer to initial and final impulse conditions. Subscript t refers to transfer orbit conditions.

For transfers with a central angle of $(2n+1)\pi$ rad (180 deg, 540 deg, . . .) Eq. (10) states that Δv_0 and Δv_f must have components normal to the transfer plane of opposite signs and inversely proportional to the respective radius magnitudes. As shown in Fig. 5, the unit angular momentum vectors h_0 , h_i , and h_f are all coplanar. Solution requires a single parameter iteration to select the transfer plane inclination so that Eq. (10) is satisfied.

Figure 6 shows the situation for $2n\pi$ transfers (0 deg, 360 deg, 720 deg, . . .). In this case $r_0=r_f=r$, and Eq. (11) expresses the same geometric constraint as Eq. (10). Since the initial, final, and transfer orbits all contain r , the unit angular momentum vectors h_0 , h_f , h_i are again coplanar. Since the transfer time is a known integer multiple of the period, the semimajor axis of the transfer ellipse and, consequently the velocity magnitude at radius $r=r_0=r_f$ are known, $v_0^+ \equiv v_f^-$. Equation (12) states that the components of Δv_0 and Δv_f

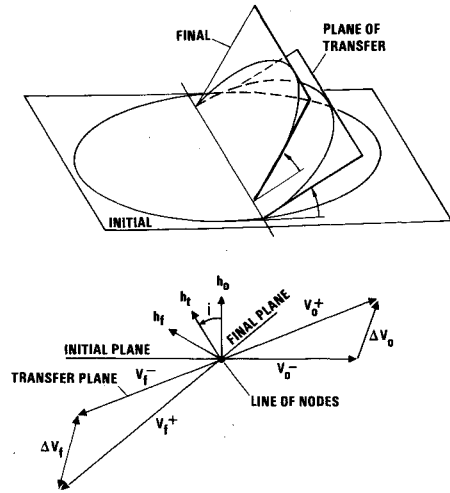


Fig. 5 Cross section of velocity diagram perpendicular to line of nodes for $(2n+1)\pi$ transfers.

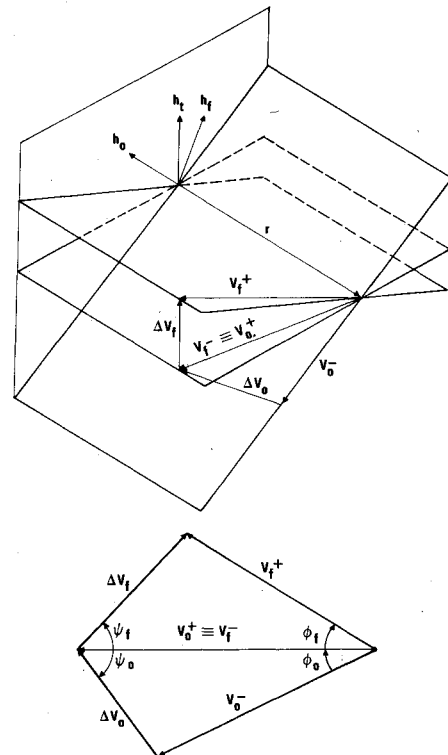


Fig. 6 Velocity diagrams for minimum delta velocity $2n\pi$ transfers.

perpendicular to both h_i and $v_0^+ \equiv v_f^-$ must be equal. An immediate consequence of Eqs. (11) and (12) is that initial, final, and transfer orbit velocities, v_0^+ , v_f^- , $v_0^+ \equiv v_f^-$ are coplanar. In addition $\psi_0 = \psi_f$ in Fig. 6 for minimum delta v transfers. Solution is obtained simply by iterating ϕ_0 until $\psi_0 = \psi_f$. ($\|v_0^+\|, \|v_f^-\|, \|v_0^+ \equiv v_f^-\| = \|v_f^-\|$, and $\phi_0 + \phi_f$ are known from the problem statement.)

Higher-Order Gravitational Harmonics

Space shuttle missions envision servicing spacecraft in geosynchronous equatorial orbit by a reusable service tug carried in the cargo bay of the space shuttle. The time required for the service tug to transfer from the shuttle's low Earth orbit to a geosynchronous orbit, service a satellite, and return to shuttle for reuse is typically several days. During the time between service tug departure and its return to the shuttle, the shuttle will have made between 30 and 100 orbital revolutions. The J_2 gravitational harmonic causes a rotation

of the longitude of the ascending node and argument of perigee of shuttle orbit of a magnitude that cannot be ignored in performance calculations. Reference 14 suggests a simple procedure for generating pseudoposition vectors that may be used in conjunction with a solution to Lambert's problem to account for second-order gravitational perturbations. Although this scheme has not been implemented by the author, it appears to be a promising approach to refining the conic approximation.

Problem Formulation

The vehicle configuration can be adequately defined by the following variables:

- W_0 = gross initial weight of the transfer vehicle and payload just before ignition of the first stage
 W_p = weight of the payload

and for each propulsion stage i

- PW_i = nominal effective main impulse propellant weight on stage i
 SPI_i = effective specific impulse of stage i
 WJ_i = weight jettisoned after stage i has expended its propellants
 O_i = propellant fraction offloaded from stage i
 S_i = a steering coefficient equal to the ratio of the net velocity imparted by an "impulse" with steering and the ideal delta velocity imparted by the stage

Vehicle performance is then computed using the following algorithms:

- a) ($i=1$) $WS = W_0$
- b) $WE = WS - PW_i(1 - O_i)$
- c) $R = WS/WE$
- d) If $R > 0$, $DV_i = gSPI_i S_i \ln R$ (13)
 If $R \leq 0$, $DV_i = 1 \times 10^{10} \max.(0.001, R)$
- e) $WS = WE - WJ_i$
- f) If this is last stage, stop; otherwise, $i = i + 1$ and go to step b.

Equation 13 is just the impulsive rocket equation, where g is surface gravitational acceleration. The weight WS defined in step e at the conclusion of the algorithm is the actual payload achieved. It is not necessarily equal to W_p , the payload weight input. In general, the variables W_0 , W_p , O_i and S_i may be treated as control variables subject to optimization.

The propellant offloading fraction may be considered a variable in the case of liquid-propellant stages, which may be tanked to optimal mission-peculiar levels. It is anticipated that the solid rocket motor for the IUS will be certified for operation within a limited range of propellant loadings. Offloading for solid rocket motors would be achieved by literally machining off part of the nominal propellant charge several months before flight. The range of allowable propellant weight reduction is limited to factors between 1.0 and 0.60, for example (exact lower bounds are to be determined). Clearly, solid-rocket-motor propellant weight is not a real-time control variable. For multiple-burn liquid-propellant stages, the nominal propellant loading may be associated with each burn subject to the constraint that $\Sigma O_i \leq 1$ over burns using the common physical stage. The offloading fraction O_i is used as a control variable rather than the propellant weights themselves as a convenience that avoids control variable scaling.

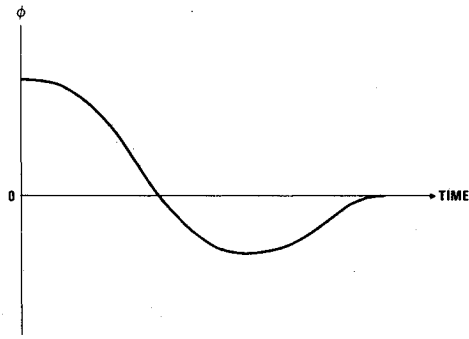


Fig. 7 Cross-axis steering angle ϕ as function of time for energy management.

The steering coefficients S_i are used to simulate cross-axis steering, which may be used as an energy management technique when a stage, carrying a fixed or minimum propellant loading, provides a larger velocity increment than the optimal increment desired. The technique consists of steering to both sides of the direction in which the velocity increment is desired so that the increments perpendicular to the desired axis cancel, as shown in Fig. 7. The magnitude of deviations from desired increment direction controls the magnitude of the effective velocity increment. Clearly, this technique is not applicable to spin-stabilized stages or to stages unable to vary attitude during a burn. S_i , of course, must be constrained to be between 0 and 1.

The initial total vehicle weight is frequently a control variable, for example when the payload weight or the propellant offloading is subject to optimization. If the payload weight is fixed or is to be constrained when either the total initial weight of the vehicle W_0 or any of the propellant offloadings O_i is an optimization variable, the input payload W_p must be input and a constraint imposed of the form $WS = W_p$ or $WS \geq W_p$ where WS is the actual final weight determined from step e at algorithm termination. Otherwise, payload weight is completely determined by the invariant weights of the problem statement.

The actual implementation has additional control variables to simulate the weight and propulsive effects of such secondary liquid systems as reaction control, propellant settling, or velocity error correction systems. Ignoring these variables, a summary of the set of available variables from which the control variables for a particular problem may be chosen is given below:

$$C = [W_0, W_p, v_0, r_0, \Delta t_0, O_i, S_i, (i=1, 2, \dots, n_b);$$

$$r_i, (i=2, 3, \dots, n_b); v_f] \quad (14)$$

where n_b = the number of burns modeled.

This Lambert problem formulation requires that the user enforce constraints of the form

$$DV_i = \|\Delta v_i\| \quad (i=1, 2, \dots, n_b) \quad (15)$$

where DV_i is determined from step d of the vehicle performance algorithm and is the "velocity provided" by stage i in its current dry weight and propellant weight configuration and $\|\Delta v_i\|$ is the "velocity required" by the solution to Lambert's problem, given the current position vectors, transfer times, and initial and final velocity vectors. Problem solution depends upon the control variables being adjusted so that constraints of Eq. (15) are satisfied.

Given the times, position vectors, velocity vectors, and Δv vectors from the solution to Lambert's problem and the DV_i and weights from the vehicle performance algorithm, a plethora of dependent variables may be computed, including orbital elements, thrust pointing angles, Earth tracker angles,

Table 1 Typical IUS stage characteristics for two example missions

Mission	Stage	Effective nominal propellant weight, lb	Effective specific impulse	Jettison weight, lb	Max. total weight, lb	Nominal payload weight, lb
PL22A 1985	1	22,500	296	2350	58,720	1125
	2	22,500	296	2740		
	3	6250	296	790		
EO56	1	22,800	297	2680	55,790	5010
	2	22,800	297	2260		
	3	6250	297.5	2156		

sun angles, and Earth impact points. Given thrust levels or propellant flow rates, actual starting times and burnout times of the finite burns and corresponding coast times may be computed.

Problem Solution

To obtain maximum flexibility in problem formulation, it is desirable to be able to select any of these dependent variables at the end of any burn or any of the control variables as the performance criterion to be optimized. It is equally desirable to be able to impose equality or inequality constraints on the same set of variables. The following nonlinear programming formulation realizes this flexibility:

$$\begin{aligned} &\text{minimize } I(x) \\ &x \end{aligned} \quad (16)$$

subjected to

$$h(x) = 0 \quad (17)$$

$$g(x) \geq 0 \quad (18)$$

where

- x = a suitable subset of the set of control variables C defined in Eq. (14); these are the variables which are free to be optimized
- h = a vector of equality constraints to be enforced including those of Eq. (15); elements of h may be control variables or any of the dependent variables which may be computed in the manner previously discussed, given the control vector x
- g = a vector of inequality constraints; as in the equality constraint case any control variable or any of the dependent variables may be so constrained

Other Solution Techniques

Approaches to the solution of impulsive orbital transfer problems may be conveniently divided into two groups: 1) indirect solution techniques that depend upon the necessary and sufficient conditions of the calculus of variations; and 2) direct solution techniques, which depend upon direct comparison of values of the problem functions for varying control vector values. An enormous body of literature has built up regarding the former approach based on Lawden's "primer vector" theory.¹⁵ References 15-21 represent only a few of the available references in this area. Indirect techniques based on the calculus of variation (Maximum Principle) are complicated by the introduction of equality and inequality constraints because of the discontinuities introduced in the adjoint functions.^{4,22} This is especially true for the case of multiple inequality constraints that may or may not be active. In addition program development and modification costs are higher for the primer vector approach than for direct approach taken in this paper.^{4,22} In general, however, the indirect approaches are computationally faster than direct techniques, when they converge.

The method of solution presented in the next section falls into the category of direct solution techniques. Relatively few publications have appeared dealing with the application of direct solution techniques to impulsive trajectory optimization. The papers of Gruver and Engersbach^{22,23} apply a gradient projection-restoration algorithm to solve the nonlinear programming problem, Eqs. (16-18). The paper of Johnson²⁴ uses a two-phased, accelerated gradient method; in the first phase, a penalty function is minimized and in the second phase the Hessian developed from the quasi-Newton function minimization of the first phase is used to perform a Newton iteration on the "active" constraints. Both approaches propagate trajectories using the Kepler problem formulation rather than the Lambert problem formulation proposed here. These papers show how analytic gradients of the performance index and constraints may be computed. This approach requires coding first partial derivatives of the constraints with respect to the state variables and is advantageous when constraints are a simple function of the state variables. However, several important constraints (e.g. tracker elevation angles, instantaneous impact latitude and longitude, and outgoing asymptote declination and right ascension) are sufficiently complicated functions of state that their first partials are, to say the least, cumbersome.

Method of Multipliers

In this section a different approach to the solution of the nonlinear programming problem is selected—one that experience has shown to be faster and more robust than penalty function approaches. Most numerical techniques for solving the above problem, which make use of gradient information, fall into one of three categories:

1) Lagrange multiplier techniques²⁵⁻³⁶ that adjoin the constraints to the objective function, using Lagrange multipliers; seek to minimize the augmented objective function with respect to the independent variables; and select Lagrange multipliers that satisfy constraints.

2) Feasible direction and gradient projection techniques^{37,38} in which successive linear search directions are chosen to satisfy constraints to the first order.

3) Penalty function techniques^{39,40} in which penalty terms are added to the function to be minimized so that a series of unconstrained minimizations of penalty functions solves the original constrained problem.

There are advantages and disadvantages to each method; choice should depend on the number of variables and constraints and the degree of nonlinearity of the constraints. Feasible direction and gradient projection techniques, although analytically complex compared to unconstrained optimization algorithms, work efficiently on problems with linear constraints. However, these methods considerably increase computation time and algorithm complexity when the constraints are highly nonlinear. Penalty function methods are easy to implement, directly admitting the use of efficient quasi-Newton methods of unconstrained function minimization; nevertheless, they require penalty terms to approach an infinite magnitude in certain regions, which

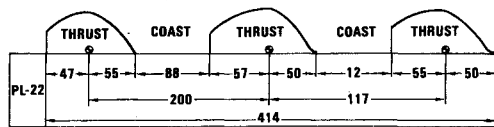


Fig. 8 Typical profile of thrust acceleration vs time for a planetary mission.

severely distorts the shape of the penalty function, inherently slowing convergence and introducing numerical problems.

The method of solution selected involves Lagrange multipliers and hence belongs to the first category of solution methods. To date, these approaches have received considerably less attention than the other two approaches. These methods avoid the severe functional distortion inherent in the penalty function approaches (and thus, the associated slowing of convergence and numerical problems) and admit the use of efficient quasi-Newton methods of function minimization. Moreover, since they do not require return to a feasible solution after each optimization step, as do feasible direction and gradient projection methods, computational load is reduced.

A variation of the Method of Multipliers originally proposed by Hestenes²⁵ was implemented to solve the nonlinear programming problem posed by Eqs. (16-18). An algorithmic presentation of this method of solution as applied to launch vehicle trajectory optimization may be found in Ref. 4. The same package of subroutines was used in both applications, indicating the flexibility and robustness of the solution technique.

Interim Upper Stage Examples

The Interim Upper Stage (IUS) is actually a family of solid-rocket-motor upper stages designed around two new solid rocket motors (SRM). The family of stages will be used to transfer payloads from the low Earth orbit of the space shuttle into higher-energy orbits; e.g., synchronous equatorial missions and planetary missions. Table 1 presents typical parameters for two proposed NASA missions presented as examples.

Pioneer Saturn/Uranus/Titan Probes Mission

The first mission is the 1985 Pioneer Saturn/Uranus/Titan Probes mission, PL-22A. The IUS must transfer the spacecraft from a 160-n. mi. altitude circular space shuttle parking orbit with an inclination of 28.31 deg onto a hyperbolic trajectory with a vis-visa energy of $C_3 = 143 \text{ km}^2/\text{s}^2$ and an outgoing asymptote declination of -3 deg . For planetary injection missions, it is desirable to execute the burns in as rapid a succession as possible. Unfortunately, this desire conflicts with the rather long thrust tailoff characteristics of solid rocket motors and the limited thrust available from reaction control systems used to achieve the minimum separation distance required for ignition of the next stage. Figure 8 shows some typical thrust vs time profiles for this mission, with thrust acceleration centroids noted.

The problem is to maximize the payload weight subject to an upper bound on the total vehicle ignition weight (due to shuttle payload capacity) and minimum coast times between stages to allow for thrust tailoff and stage separation. The control variables were total vehicle ignition weight, coast time in the space shuttle parking orbit before the first impulse, position vectors and times of the second and third impulses, velocity vector after the third impulse, and propellant offloading of each of the three stages. Thus, there are sixteen control variables. The equality constraints h consist of one impulse compatibility constraint, Eq. (15), for each of the three impulses, a final energy, and a final declination constraint for a total of five equality constraints. The inequality constraints consist of an upper bound on the total vehicle ignition weight, upper and lower bounds on the offloading of

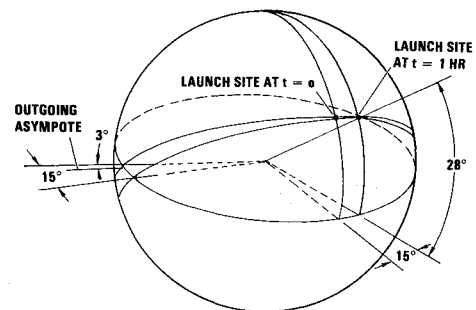


Fig. 9 Launch window performance geometry.

each stage, and lower bounds on the two coast times separating the three stages for a total of nine inequality constraints. The offloadings for each stage were bounded between 0.0 and 0.4 of the maximum propellant loads.

A solution accurate to six significant figures was obtained in between 80 and 120 s of central processor time on the CDC CYBER 172 computer, depending on the initial solution estimate. For this problem each one-dimensional search of the unconstrained function minimization required approximately 1.3 s. The complete evaluation of a single trajectory, including evaluation of more than 70 dependent variables after each impulse of the trajectory (orbital parameters, weights, etc.), required less than 0.06 s.

The optimal total vehicle ignition weight was 58,557 lb, 163 lb under the maximum space shuttle capacity for this mission. Each solid rocket motor was fully loaded, resulting in a payload weight of 1427 lb—well above the nominal payload weight. The initial IUS position was assumed to be directly over Cape Canaveral with a latitude of 28.31 deg and a longitude of 279.46 deg. The centroid of the first-stage burn occurred at a latitude of -21.98 deg and a longitude of 58.00 deg after a 7576 s coast. As expected, each of the next two impulses occurred at the earliest possible time consistent with the minimum coast time constraints. The optimal average thrust pointing direction for each stage was -7.4 deg , 1.8 deg , and 10.2 deg , respectively, above the local horizontal. The thrust vectors were contained in the orbital plane for each stage. The resulting inertial right ascension of the outgoing asymptote was 183.86 deg relative to the prime meridian at time 0.

The solution ignores part of the launch day planetary geometry by assuming that the space shuttle parking orbit is selected to contain the outgoing hyperbolic asymptote at the time of the spacecraft injection. This requires that the space shuttle be launched at a precise time each day when the plane defined by the outgoing asymptote (fixed in inertial space) and the radius vector to the launch site (rotating with the Earth) has the desired predetermined inclination. The alternative of launching into parking orbits with time-varying inclinations, requiring time-varying launch azimuths, is considered undesirable from the range safety considerations (tank re-entry) and space shuttle SRM recovery considerations. Further, launch at a precise time of a complex vehicle such as the space shuttle cannot be guaranteed due to safety precautions that occasionally result in last-minute holds. The usual practice is to attempt launch within some "window" containing the desired launch time. One-hour launch windows are typical.

Launch at a time other than the desired time results in a space shuttle orbital plane that does not contain the outgoing asymptote. An important part of mission analysis then is to determine the optimal transfers for these nonplanar cases and to quote the resulting performance degradation as a function of time through the launch window. This is easily done by noting the inertial right ascension of the outgoing asymptote (relative to the prime meridian at time 0.) for the optimal (planar) trajectory. Then, solve the same problem assuming the vehicle is over Cape Canaveral at a different time, say 30

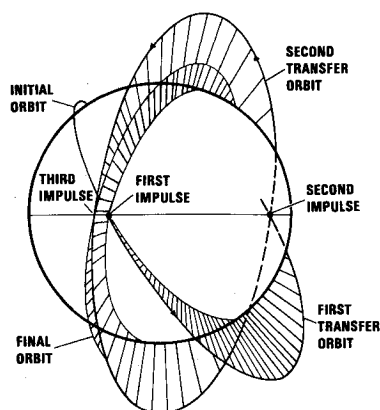


Fig. 10 Three-burn environmental monitor satellite transfer from Eastern Test Range (ETR). Also see Table 2.

Table 2 Orbital parameters for three-burn insertion from ETR

	Apogee, n. mi.	Perigee, n. mi.	Inclination, deg.
Initial orbit	140	140	57.0
1st transfer orbit	2466	140	61.6
2nd transfer orbit	2466	900	93.5
Final orbit	900	900	103.0

min later at time = 1800 s with the same inclination. This results in an initial inertial longitude of 286.98 deg (relative to the prime meridian at time 0.) due to the Earth's rotation. But now add the additional constraint that the outgoing asymptote must have the same inertial right ascension (relative to the prime meridian at time 0.) as determined by the initial case. The geometry for this mission is shown in Fig. 9. The optimal solution for this case resulted in the first burn occurring approximately 100 s earlier than in the planar case and thrusting out of the orbital plane for each of the burns. The payload capability was reduced by 40 lb.

Environmental Monitor Satellite

The second example mission is the Environmental Monitor Satellite, EO-56 of the NASA Mission Model. The objective is to place the maximum payload into a 900-n. mi. circular parking orbit at an inclination of 103 deg. This is a Sun-synchronous orbit, meaning that the longitude of the ascending node revolves at the same rate as the Earth revolves about the Sun.

The mission can easily be flown out of the Western Test Range. However, at one time space shuttle launches out of the Western Test Range were in question, and mission analysis was performed assuming a launch from Cape Canaveral at the most northerly permissible azimuth for space shuttle launch. This results in an initial circular space shuttle parking orbit with an altitude of 140-n. mi. and an inclination of 57 deg. The orbital transfer thus requires a challenging orbital plane change of 46 deg. Characteristics of one vehicle configuration considered for this mission are presented in Table 1. For this mission, the offload fractions were restricted to be between 0.0 and 0.40. The control vector was the same as for the PL-22 mission. The equality constraints h consisted of the delta velocity compatibility constraint, Eq. (15), for each of the three stages and the apogee, perigee, and inclination of the final orbit for a total of six constraints. The inequality constraints g were an upper bound on the total vehicle ignition weight, upper and lower bounds on the offloading for each of the stages, and a lower bound on the payload weight for a total of eight inequality constraints.

A solution accurate to four significant digits required 141 s of central processor time on a CDC CYBER 172 computer.

The geometry of the solution is shown in Fig. 10 and Table 2. As before, the IUS is assumed to be directly over Cape Canaveral at time = 0. After a 2173-s coast, the first impulse at a latitude of 0.15 deg and an inertial longitude of 78.88 deg places the IUS in an elliptical orbit with an apogee of 2466 n. mi., a perigee of 140 n. mi., and an inclination of 61.6 deg. Near the apogee and the ascending node, the primary plane change maneuver occurs, resulting in an elliptical orbit with an apogee of 2466 n. mi., a perigee of 900 n. mi., and an inclination of 93.5 deg. As might be expected, injection into the final orbit occurs at the descending node. The optimal propellant offloadings were: 0.224 for the first stage, 0.0 for the second stage, and the maximum allowable offloading, 0.40, for the third stage. The total vehicle ignition weight was also at its maximum value. The resulting payload weight was 4496 lb, 514 lb short of the desired payload weight. It is currently planned to launch this mission out of the Western Test Range.

These examples show only a small portion of the power and flexibility of this approach. To date, problems with 7 impulses, 35 control variables, and 31 constraints have been successfully solved. Most recently, an analytic booster model has been incorporated in the program, called CONITO, to allow simulation of complete missions from the ground up. The solution times are sufficiently short to allow problem solution in an interactive mode using a remote terminal on prime shift time.

Conclusions

The combination of the impulsive thrusting approximation, the solution to Lambert's problem for coasting arcs, and a variation of the Methods of Multipliers for nonlinear programming, has resulted in a rapid and reliable tool for the determination of optimal space trajectories subject to complex practical constraints. A Lambert problem formulation was chosen over a Kepler problem formulation because of numerical conditioning and stability considerations as well as ease of use. However, care must be taken in developing an algorithm to solve Lambert's problem to account for solution ambiguities inherent in the formulation. The basic solution strategy proposed in this paper adapts easily to other problems and complex constraints.

Acknowledgment

This paper was presented as Paper 77-216 at the 28th International Astronautical Federation Congress, Prague, Czechoslovakia, Sept. 25-Oct. 1, 1977.

References

- Denham, W.F. and Bryson, A.E., "Optimal Programming Problems With Inequality Constraints II: Solution by Steepest-Ascent," *AIAA Journal*, Vol. 2, Jan. 1964, pp. 25-34.
- Speyer, J. L., Kelley, H.J., Levine, N., and Denham, W. F., "Accelerated Gradient Projection Techniques With Application to Rocket Trajectory Optimization," *Automatica*, Vol. 7, Jan. 1971, pp. 37-43.
- Edge, E.R. and Powers, W.F., "Shuttle Ascent Trajectory Optimization with Function Space Quasi-Newton Techniques," *AIAA Journal*, Vol. 14, Oct. 1976, pp. 1369-1376.
- Brusch, R. G., "Trajectory Optimization for The Atlas/Centaur Launch Vehicle," *Journal of Spacecraft and Rockets*, Vol. 14, Sept. 1977, pp. 550-555.
- Gobet, F. W. and Doll, J.R., "A Survey of Impulsive Trajectories," *AIAA Journal*, Vol. 7, May 1969, pp. 801-834.
- Robbins, H.M., "An Analytic Study of the Impulsive Approximation," *AIAA Journal*, Vol. 4, Aug. 1966, pp. 1417-1423.
- Goodyear, W.H., "Completely General Closed Form Solution for Coordinates and Partial Derivatives of the Two-Body Problems," *Astronomical Journal*, Vol. 10, April 1965, pp. 189-192.
- Goodyear, W.H., "A General Method for the Computation of Cartesian Coordinates and Partial Derivatives of the Two-Body Problem," NASA CR-522, Sept. 1966.
- Battin, R. H., "Lambert's Problem Revisited," *AIAA Journal*, Vol. 15, May 1977, pp. 707-713.

- ¹⁰Battin, R. H., "A New Solution for Lambert's Problem," *Proceeding of the XIXth International Astronautical Congress*, Vol. 2, Pergamon Press, PWN-Polish Scientific Publishers, 1970, pp. 131-150; also see *Space Guidance and Navigation*, AIAA Professional Study Series, pp. 199-216.
- ¹¹Rocklin, S. M., "A Study of the Singularities of the Primer Vector," Masters Thesis, Princeton University, Princeton, N. J., 1967.
- ¹²Roberts, P. H., "ORBIT, An Improved Set of Subroutines," Jet Propulsion Laboratories, Pasadena, Calif., Tech. Memo. 393-114, Oct. 1972, pp. 1-14.
- ¹³Stoer, J. and Bulirsch, R., *Enfuehrung in die Numerische Mathematik II (Introduction to Numerical Mathematics II)*, Springer-Verlag, New York, 1973, pp. 151-191.
- ¹⁴Uphoff, C., Roberts, P. H., and Friedman, L. D., "Orbit Design Concepts for Jupiter Orbiter Missions," *Journal of Spacecraft and Rockets*, Vol. 13, June 1976, pp. 348-355.
- ¹⁵Lawden, D. F., *Optimal Trajectories for Space Navigation*, Butterworths, London, 1962.
- ¹⁶Lion, P. M. and Handelsman, M., "Primer Vector on Fixed-Time Impulsive Trajectories," *AIAA Journal*, Vol. 6, Jan. 1968, pp. 127-132.
- ¹⁷Hazelrigg, G. A., "Analytic Determination of the Adjoint Vectors for Optimum Space Trajectories," *Journal of Spacecraft and Rockets*, Vol. 7, Oct. 1970, pp. 1200-1207.
- ¹⁸Hazelrigg, G. A., "Optimal Interplanetary Trajectories for Chemically Propelled Spacecraft," *Journal of Spacecraft and Rockets*, Vol. 8, Sept. 1971, pp. 915-919.
- ¹⁹Jezewski, D. J., "Optimal Analytic Multiburn Trajectories," *AIAA Journal*, Vol. 10, May 1972, pp. 680-685.
- ²⁰Jezewski, D. J., "N-Burn Optimal Analytic Trajectories," AIAA Paper 72-929, AIAA/AAS Astrodynamics Conference, Palo Alto, Calif., Sept. 1972.
- ²¹Betts, J. T., "Optimal Three Burn Orbit Transfer," *AIAA Journal*, Vol. 15, June 1977, pp. 861-864.
- ²²Gruver, W. A. and Engersbach, N., "A Mathematical Programming Approach to the Optimization of Constrained Impulsive, Minimum Fuel Trajectories," Institut fur Dynamik der Flugsysteme, Oberpfaffenhofen, West Germany, Report IB 013-72/3, June 1972, pp. 1-30.
- ²³Gruver, W. A. and Engersbach, N. H., "Nonlinear Programming by Projection-Restoration Applied to Optimal Geostationary Satellite Positioning," *AIAA Journal*, Vol. 12, Dec. 1974, pp. 1715-1720.
- ²⁴Johnson, I. L., "Impulsive Orbit Transfer Optimization by an Accelerated Gradient Method," *Journal of Spacecraft and Rockets*, Vol. 6, May 1969, pp. 630-632.
- ²⁵Hestenes, M. R., "Multiplier and Gradient Methods," *Journal of Optimization Theory and Applications*, Vol. 4, Nov. 1969, pp. 303-320.
- ²⁶Powell, M. J. D., "A Method for Nonlinear Constraints in Minimization Problems," in *Optimization*, edited by R. Fletcher, Academic Press, London, England, 1969.
- ²⁷Hazelrigg, G. A., Brusch, R. G., and Sachs, W. L., "Optimal Space Trajectories with Delta Velocity Constraints," *Proceedings of the 21st International Astronautical Congress*, North Holland Publishing Co., Amsterdam, 1971.
- ²⁸Haarhoff, P. C. and Buys, J. D., "A New Method for the Optimization of a Nonlinear Function Subject to Nonlinear Constraints," *The Computer Journal*, Vol. 13, May 1970, pp. 178-184.
- ²⁹Nahra, J. E., "Balance Function for the Optimal Control Problem," *Journal of Optimization Theory and Applications*, Vol. 8, July 1971, pp. 35-48.
- ³⁰Merriam, C. W., "Improved Second-Order Methods for Solving Constrained Parameter Optimization Problems Arising in Control," *International Journal of Control*, Vol. 15, May 1972, pp. 865-876.
- ³¹Miele, A., Moseley, P. E., Levy, A. V., and Coggins, G. M., "On the Method of Multipliers for Mathematical Programming Problems," *Journal of Optimization Theory and Applications*, Vol. 10, Jan. 1972, pp. 1-33.
- ³²Buys, J. D., "Dual Algorithms for Constrained Optimization Problems," Ph.D. dissertation, University of Leiden, Netherlands, June 1972.
- ³³Brusch, R. G., "A Rapidly Convergent Method of Equality Constrained Function Minimization," *IEEE Conference on Decision and Control*, San Diego, Calif., Dec. 5-7, 1973.
- ³⁴Kort, B. W. and Bertsekas, D. P., "Multiplier Methods for Convex Programming," *IEEE Conference on Decision and Control*, San Diego, Calif., Dec. 5-7, 1973.
- ³⁵Bertsekas, D. P., "Multiplier Methods: A Survey," *Automatica*, Vol. 12, March-April 1976, pp. 133-145.
- ³⁶Brusch, R. G., "A Numerical Comparison of Several Multiplier Methods," *IEEE Conference on Decision and Control*, Phoenix, Ariz., Dec. 1974.
- ³⁷Zoutendijk, G., *Methods of Feasible Directions*, Elsevier Publishing Co., Amsterdam, Holland, 1960.
- ³⁸Rosen, J. B., "The Gradient Projection Method for Nonlinear Programming, Part II: Nonlinear Constraints," *SIAM Journal*, Vol. 9, 1961, pp. 514-532.
- ³⁹Kelley, H. J., "Method of Gradients," in *Optimization Techniques*, edited by G. Leitmann, Academic Press, New York, 1962.
- ⁴⁰Fiacco, A. V. and McCormick, G. P., *Nonlinear Programming: Sequential Unconstrained Minimization Techniques*, John Wiley & Sons, Inc., New York, 1968.